technische universität dortmund

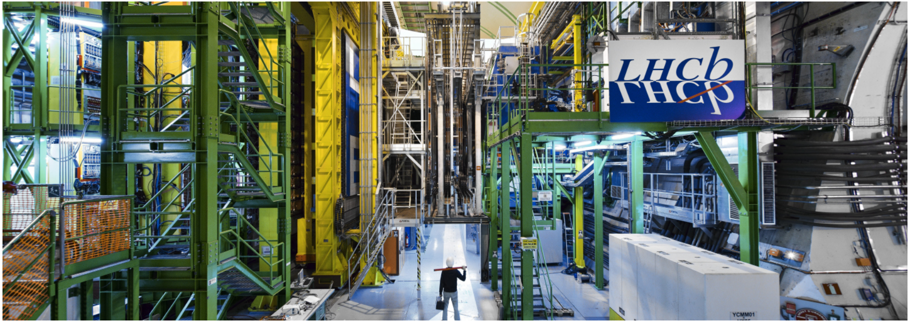

Measurement of strangeness production in pNe collisions at LHCb

Theodor Zies

IMAPP final examination, 29.09.2025

Collaboration: Johannes Albrecht, Noah Behling, Felix Riehn (TU Dortmund)
Chiara Lucarelli, Saverio Mariani (CERN)

Cosmic rays

- Cosmic rays, highly energetic particles coming from the universe
- Energies of up to 10^{20} eV
- Cosmic ray composition unknown, but needed to learn more about origins of highly energetic particles

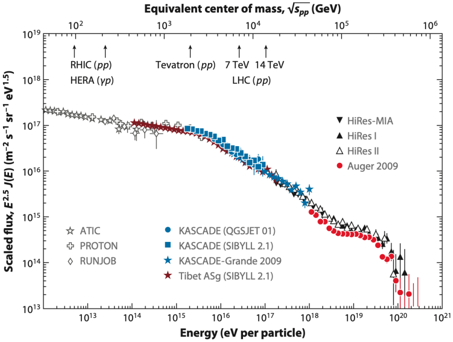

Image source: Extensive Air Showers and Hadronic Interactions at High Energy, R. Engel et al., Annu. Rev. Nucl. Part. Sci 61 (2011) 467.

Air showers

- Indirect measurements of the cosmic ray spectrum using air showers
- Extensive air showers caused by interactions of cosmic rays with the atmosphere of the Earth
- Ground-based obervatories, e.g. Pierre Auger Observatory
- Reconstruct energy of primary particle via shower depth and number of muons
- Need effective, data-driven models of hadronic interactions to simulate air showers
  →e.g. EPOS-LHC, QGSJet

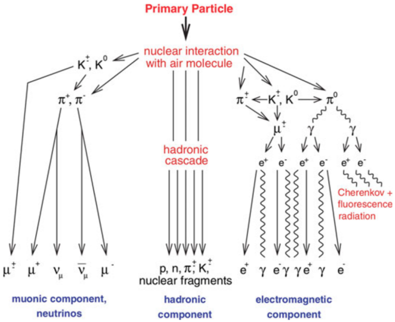

Image source: Introduction to Cosmic Rays and Extensive Air Showers, In: Emission of Radio Waves in Particle Showers, Zilles, A. (2017)

The muon puzzle

- Simulations predict too few muons at high energies →muon puzzle
- Proposed solution of muon puzzle: strangeness enhancement
- Observed by ALICE in high-multiplicity events at central pseudorapidity
- Search for enhanced strangeness production in rapidity region relevant for air showers →LHCb experiment
- Test predictions of hadronic interaction models

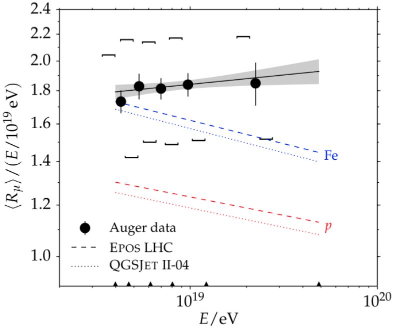

Image source: Muons in air showers at the Pierre Auger Observatory: Mean number in highly inclined events, Pierre Auger Collaboration, Phys. Rev. D 91, 032003 (2015)

The LHCb experiment

- One of four main experiments at the Large Hadron Collider at CERN
- Single-arm forward spectrometer covering $2 < \eta < 5$
- Designed to study CP violation, rare decays of b and c hadrons, and flavor oscillations
- Forward layout allows fixed-target physics with SMOG system
- Many improvements in LHCb Upgrade 1, including newly designed SMOG2
- Tracking system completely renewed, hardware trigger removed

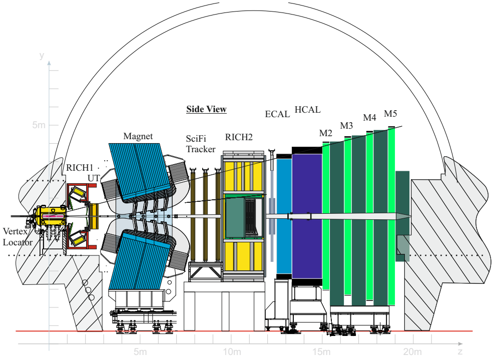

Image source: The LHCb Upgrade I, LHCb collaboration, JINST 19 (2024) P05065

The SMOG2 system

- Original SMOG: Inject noble gases into the beam pipe around the VELO
  →Designed for luminosity measurements
- Updated SMOG2: Standalone gas storage cell integrated into upgraded VELO
- Increased areal gas density, more gas species
- Fixed-target and collider physics performed in parallel

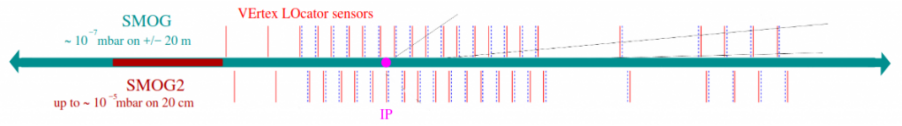

Image source: More on the SMOG system, LHCb outreach

Analysis overview

- Fixed-target collisions collected using SMOG2
  →Closest match to oxygen in Run 3 data: neon

1. Data sample:
   - pNe collisions in Run3 (2024) with SMOG2
   - $\sqrt{s_{\text{NN}}} = 113$ GeV, $\mathcal{L}_{\text{int}} = 225\,\text{nb}^{-1}$
   - Contains $\Lambda^0 \to p\pi$ and $K^0_S \to \pi\pi$ candidates
2. Simulation sample:
   - 10M minimum bias pNe and ppNe events

- Goal: Measure $R(\Lambda^0, K^0_S)$ and $R(\Lambda^0, \bar{\Lambda}^0)$ ratios in bins of p_T and y^*
  →Compare with EPOS-LHC and QGSJet predictions

$$R(\Lambda^0, K^0_S) = \frac{\sigma(pp \to \Lambda^0 X)}{\sigma(pp \to K^0_S X)} = \frac{N(\Lambda^0 \to p\pi^-)\varepsilon_{K^0_S \to \pi^+\pi^-}\mathcal{B}(K^0_S \to \pi^+\pi^-)}{N(K^0_S \to \pi^+\pi^-)\varepsilon_{\Lambda^0 \to p\pi^-}\mathcal{B}(\Lambda^0 \to p\pi^-)}$$

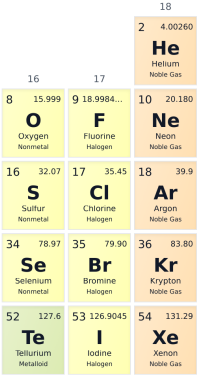

Image source: National Center for Biotechnology Information (2025). Periodic Table of Elements.

Crossfeed removal

- Checked crossfeed from K_S^0 to Λ^0 and vice versa by substituting mass hypotheses: $m_{\text{inv}}(p,\pi)|m_p \to m_\pi$ for Λ^0 and $m_{\text{inv}}(\pi,\pi)|m_\pi \to m_p$ for K_S^0
- Found significant K_S^0 peak in the Λ^0 tuple
- Almost no Λ^0 signal in K_S^0 tuple
- Veto should have already been included in trigger selection, reapplied the cut

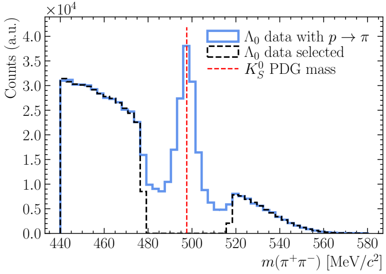

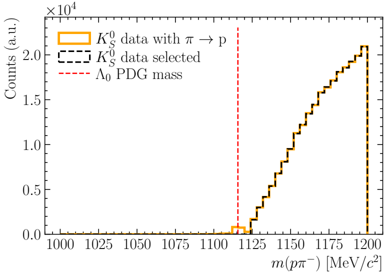

Signal yields extraction via fits

- Acquire signal yields via fits to invariant mass distributions of the Λ^0 and K^0_S candidates
- Binning scheme optimized to ensure equally populated bins
- Model: Double Crystal Ball function for signal and linear function for background

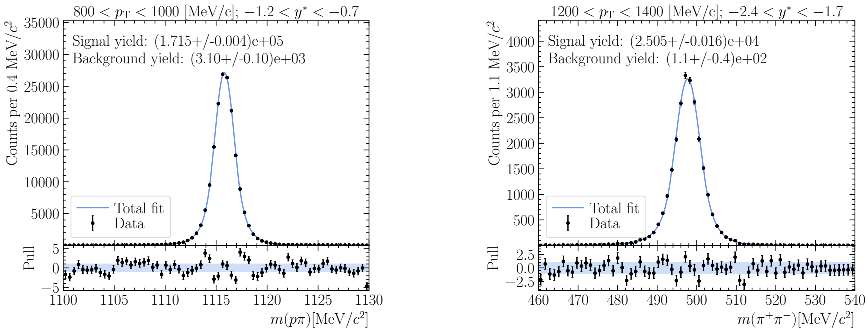

Fit uncertainty systematics

- Determine systematic fit uncertainties due to the choice of model
- Alternate models: Double Gaussian for signal, exponential for background
- Recalculate ratios using new models
- Less than 1 % systematic uncertainty

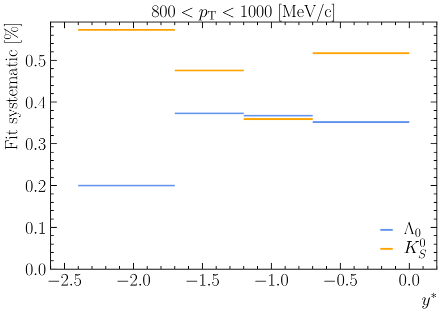

Simulation reweighting

- Kinematic variables p_T and y^* not perfectly modeled in simulation
- Efficiencies depend on binning →correction needed for unbiased efficiencies
- 2D kinematic reweighting in p_T and y^* for pNe, 3D reweighting including event multiplicity for ppNe
- Additional tracking correction determined using a pp calibration sample

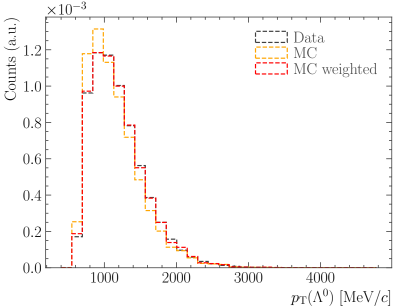

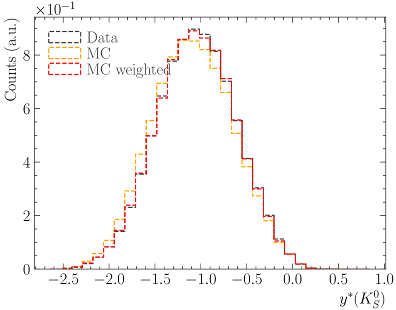

Correction for non-prompt signal contributions

- Not all Λ^0 and K_S^0 candidates are prompt, i.e. produced directly in the pNe collision
  →Determine correction factor for non-prompt signal component
- Use MC truth information in simulation to get the fraction of non-prompt signal
- Definition of non-prompt: Candidates with ancestors that have a lifetime of more than 30 ps

$$f_{\text{non-prompt}} = 1 - \frac{n_{\text{non-prompt}}}{n_{\text{total}}}$$

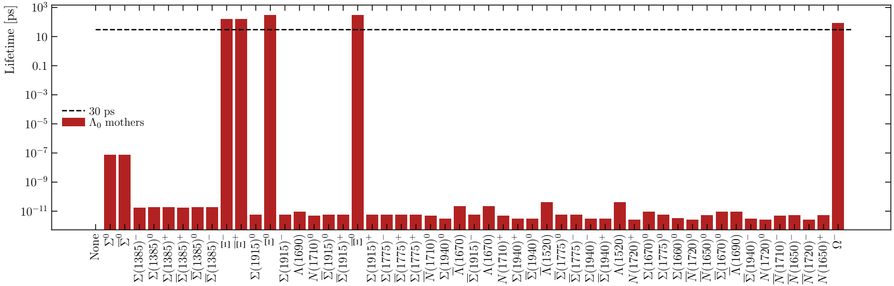

Reconstruction and trigger efficiencies

- Calculate efficiencies using simulation
- Simulation contains tuples on generator and detector level
- Applied truthmatching to the simulation, only prompt candidates and no ghost tracks
- Individually in each bin of p_T and y^*
- Statistical uncertainties due to limited simulation sample size

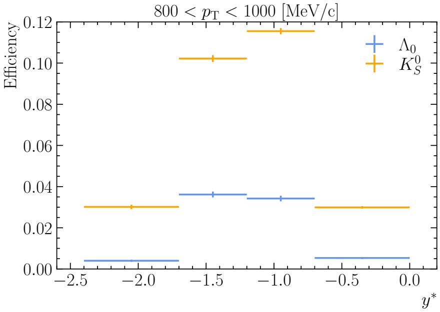

$$\epsilon_{\text{rec+trig}} = \epsilon_{\text{rec}} \cdot \epsilon_{\text{trig}} = \frac{N_{\text{rec}}}{N_{\text{gen}}} \cdot \frac{N_{\text{trig}}}{N_{\text{rec}}} = \frac{N_{\text{trig}}}{N_{\text{gen}}} \Rightarrow \frac{\sum_{\text{trig}} w_{\text{kin}} \cdot w_{\text{track}}}{\sum_{\text{gen}} w_{\text{kin}}}$$

Selection efficiencies

- Only offline selection: reapplication of mass veto
- Use simulation to determine efficiency of the selection
- Same truthmatching as before

$$\epsilon_{\text{sel}} = \frac{N_{\text{sel}}}{N_{\text{tot}}} \Rightarrow \frac{\sum_{\text{sel}} w_{\text{kin}} \cdot w_{\text{track}}}{\sum_{\text{tot}} w_{\text{kin}} \cdot w_{\text{track}}}$$

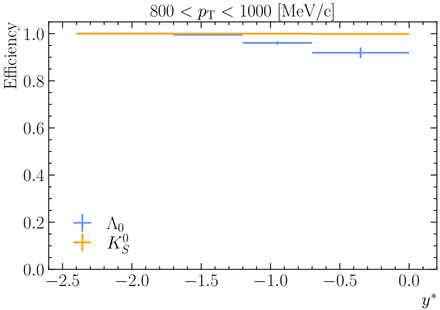

Simulation corrections (1/2)

- Simulation discards particles decaying behind the detector
- Λ^0 and K_S^0 have long lifetimes, significant fraction is affected
- Use decay time distribution to estimate number of missing candidates
- Calculate correction factor: $f_{\text{correction}} = A_{\text{Hist}}/A_{\text{Fit}}$

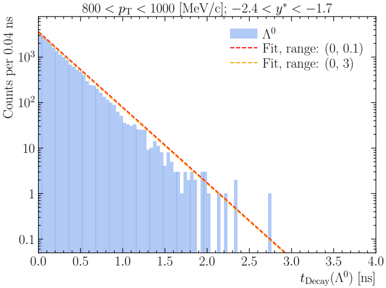

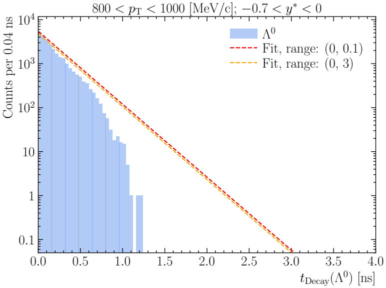

Simulation corrections (2/2)

- Poor modeling of primary vertex impact parameter in simulation
- Discrepancy worse in Λ^0 tuple
- Rescale BPVIP and $\mathrm{BPVIPCHI2}$ distributions
- Calculate efficiency correction factor from reapplying $\mathrm{HLT2}$ cut on the corrected distribution
- Less than $1\,\%$ effect

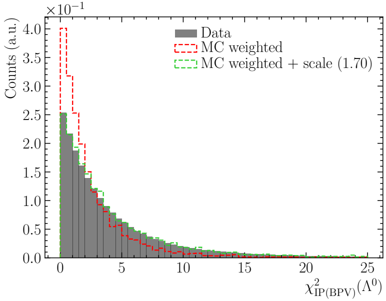

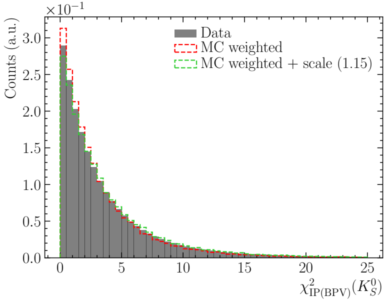

Results for the Λ^0/K^0_S ratio

- Generally observe good agreement between data and hadronic models
- EPOS-LHC not favored by data
- Newest models EPOS-LHC-R and QGSJet-III give best predictions
- Uncertainties still underestimated due to missing systematics

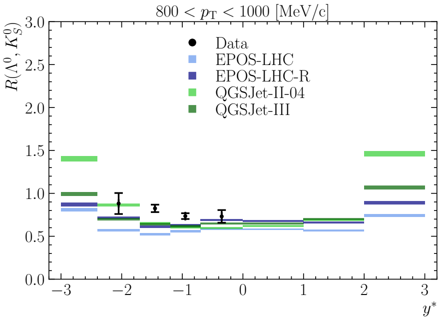

Results for the Λ^0/K^0_S ratio

- Generally observe good agreement between data and hadronic models
- EPOS-LHC not favored by data
- Newest models EPOS-LHC-R and QGSJet-III give best predictions
- Uncertainties still underestimated due to missing systematics

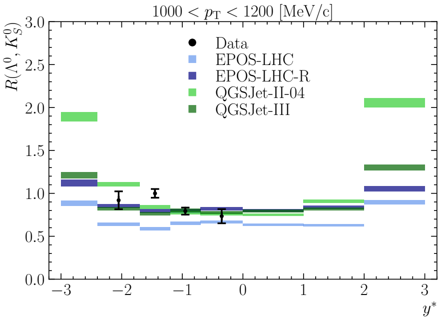

Results for the Λ^0/K^0_S ratio

- Generally observe good agreement between data and hadronic models
- EPOS-LHC not favored by data
- Newest models EPOS-LHC-R and QGSJet-III give best predictions
- Uncertainties still underestimated due to missing systematics

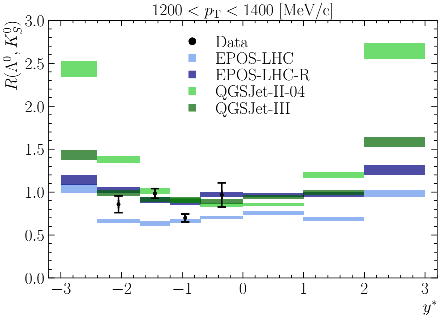

Results for the $\Lambda^0/\mathrm{K}^0_\mathrm{S}$ ratio

- Generally observe good agreement between data and hadronic models
- EPOS-LHC not favored by data
- Newest models EPOS-LHC-R and QGSJet-III give best predictions
- Uncertainties still underestimated due to missing systematics

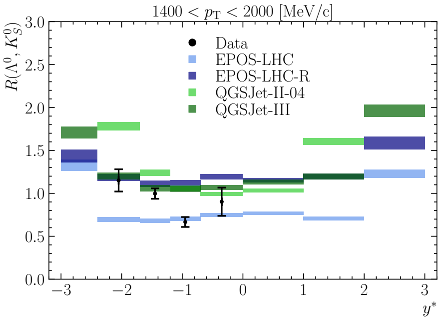

Results for the $\Lambda^0/\bar{\Lambda}^0$ ratio

- Good agreement between data and hadronic models
- Larger uncertainties due to smaller sample sizes
- Similar predictions by all hadronic models except at low rapidity

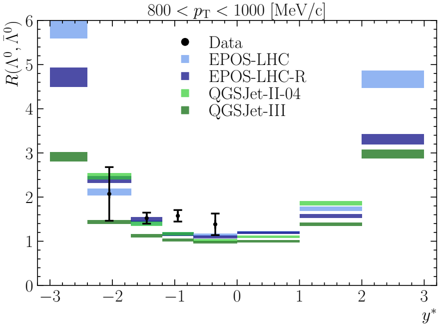

Results for the $\Lambda^0/\bar{\Lambda}^0$ ratio

- Good agreement between data and hadronic models
- Larger uncertainties due to smaller sample sizes
- Similar predictions by all hadronic models except at low rapidiy

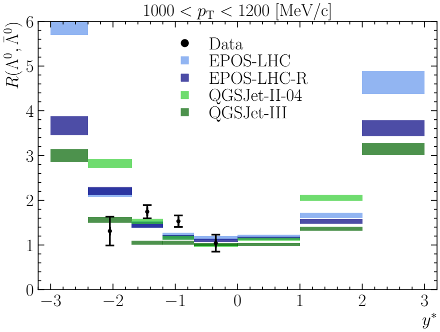

Results for the $\Lambda^0/\bar{\Lambda}^0$ ratio

- Good agreement between data and hadronic models
- Larger uncertainties due to smaller sample sizes
- Similar predictions by all hadronic models except at low rapidiy

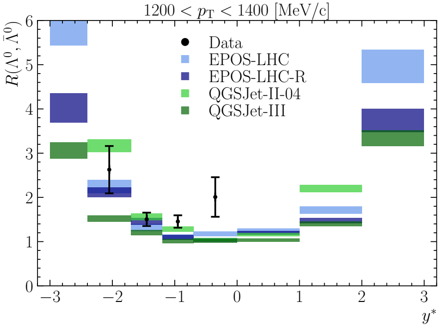

Results for the $\Lambda^0/\bar{\Lambda}^0$ ratio

- Good agreement between data and hadronic models
- Larger uncertainties due to smaller sample sizes
- Similar predictions by all hadronic models except at low rapidiy

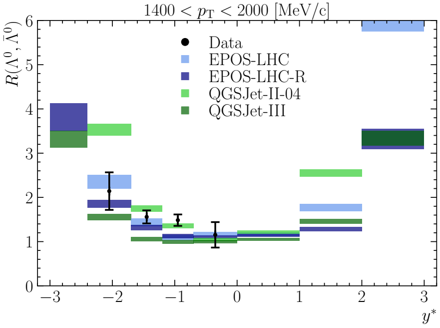

Impact of the simulation sample

- Recalculate ratios using ppNe simulation, approximately same sample size
- No systematic difference in ratios
- Significant statistical fluctuations in results compared to pNe simulation
- Simulation sample size is limiting factor in analysis

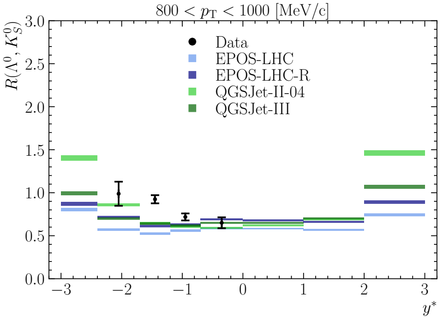

Impact of the simulation sample

- Recalculate ratios using ppNe simulation, approximately same sample size
- No systematic difference in ratios
- Significant statistical fluctuations in results compared to pNe simulation
- Simulation sample size is limiting factor in analysis

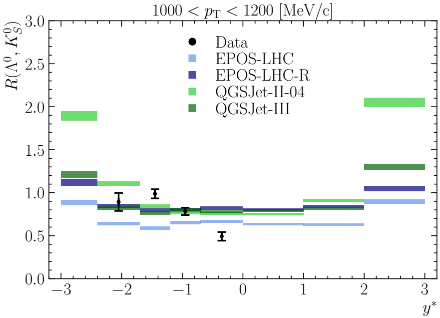

Impact of the simulation sample

- Recalculate ratios using ppNe simulation, approximately same sample size
- No systematic difference in ratios
- Significant statistical fluctuations in results compared to pNe simulation
- Simulation sample size is limiting factor in analysis

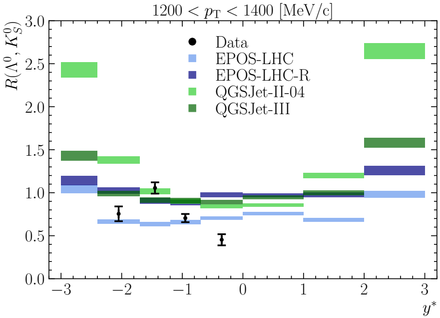

Impact of the simulation sample

- Recalculate ratios using ppNe simulation, approximately same sample size
- No systematic difference in ratios
- Significant statistical fluctuations in results compared to pNe simulation
- Simulation sample size is limiting factor in analysis

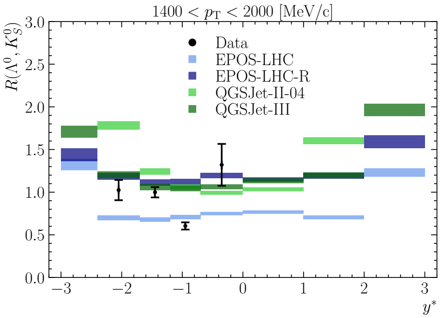

Summary

- Calculated $R(\Lambda^0, K_S^0)$ and $R(\Lambda^0, \bar{\Lambda}^0)$ using pNe collisions collected with SMOG2 in Run 3
- Compared results with different versions of EPOS-LHC and QGSJet
- Observe good agreement between data and hadronic models
- Measurement serves as input for hadronic interaction models →cosmic ray reconstruction

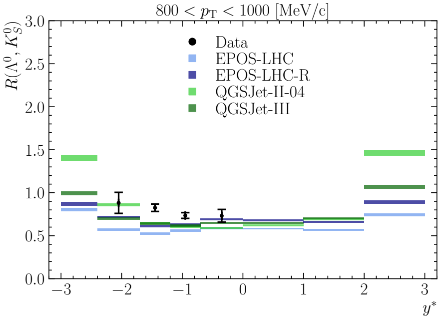

Outlook

- Missing studies of systematic uncertainties
- Limited simulation sample size
- Next steps
  1. Include heavier baryons, e.g. Ξ^0, $\Xi^\pm$, or $\Omega^\pm$
  2. Expand analysis to calculate absolute production cross-sections
  3. Probe multiplicity dependence
  4. Test other hadronic configurations and models
- New oxygen data available from special LHC runs in July 2025

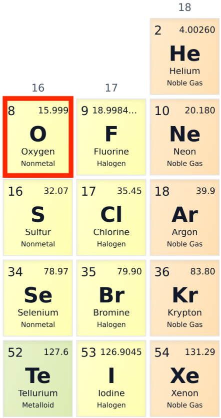

Image source: National Center for Biotechnology Information. "Periodic Table of Elements" PubChem

Thanks for your attention!

Appendix

Bonus: Oxygen runs at the LHC and pO data taking

- Special Oxygen Runs at LHC in July 2025
- LHCb collected pO and fixed-target OH_2 data with SMOG2
- Excellent data samples for air-shower physics
- Data targets greatly exceeded
- I operated the SMOG2 system during the fixed-target runs

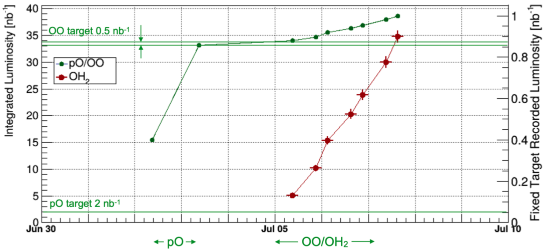

ALICE strangeness enhancement

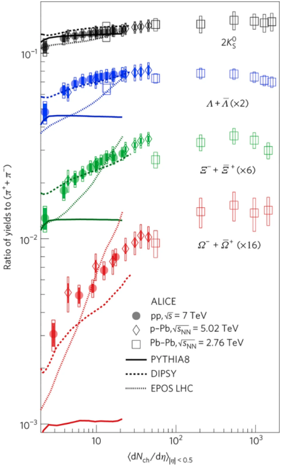

Air shower simulation

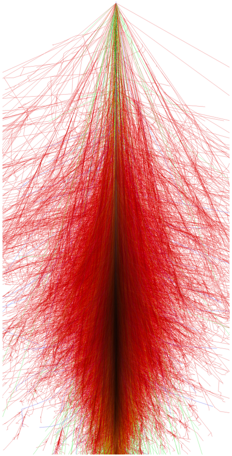

Image source: CORSIKA Shower Images: Iron Showers

SMOG2 system design

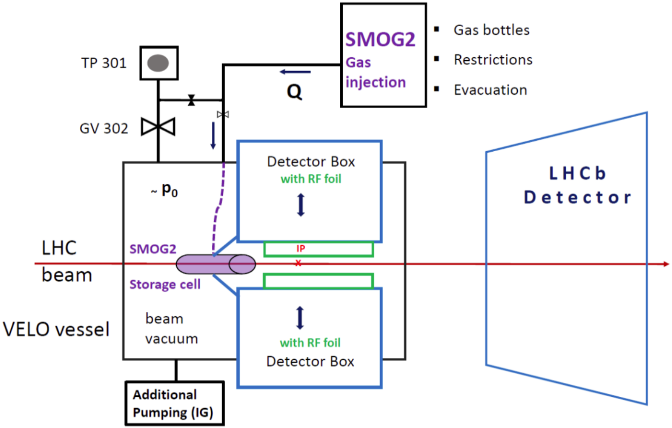

SMOG runs

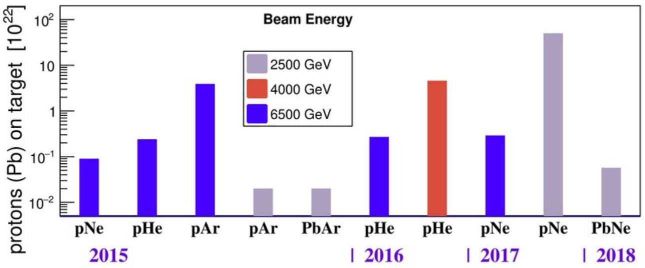
protons (Pb) on target [10^{22}]
10^2
10
1
10^{-1}
10^{-2}
Beam Energy
2500 GeV
4000 GeV
6500 GeV
pNe
pHe
pAr
pAr
PbAr
pHe
pHe
pNe
pNe
PbNe
2015
2016
2017
2018

SMOG2 HLT1 line for Λ^0

Hlt1_SMOG2_L0Toppi
$\mathrm{PV}_z > -537.5$ cm
$\mathrm{PV}_z < -337.5$ cm
$\mathrm{EV}_z > -537.5$ cm
$\chi^2_{\mathrm{VTX}} < 10$
$\mathrm{DIRA} > 0.99985$
$\chi^2_{\mathrm{IP}}(p) > 16$
$\chi^2_{\mathrm{IP}}(\pi) > 42$
$p_{\mathrm{T}}(\pi) > 150$ MeV$/c$

SMOG2 HLT1 line for K^0_S

Hlt1_SMOG2_KsPiPi
$\text{PV}_z > -537.5$ cm
$\text{PV}_z < -337.5$ cm
$p_T(\text{Track}) > 250$ MeV/c
$m(\pi^+\pi^-) > 450$ MeV/c^2
prescale $= 0.3$
postscale $= 1$

SMOG2 HLT2 line for Λ^0

Hlt2IFTFull_SMOG2Lambda02PPiLL
prescale $= 0.02$
persistreco $=$ True
$p(\Lambda^0) > 2$ GeV/c
$\chi^2_{\text{DOF}}(\text{Track}) < 5$
$\chi^2_{\text{IP}}(\text{BPV}) > 25$
$m(p\pi) > (1115.683 - 25)$ MeV/c^2
$m(p\pi) < (1115.683 + 25)$ MeV/c^2
apt > 0 MeV/c
$\chi^2_{\text{DOF}}(v) < 25.0$
$\text{EV}_z < 2200$ mm
$\chi^2(\text{BPVVD}) > 0$
$t_{\text{life}}(\text{BPV}) > 0$ ns
$\chi^2_{\text{IP}}(\text{Parent}) < 100$
VetoWindow$(K^0_S) = 20$ MeV/c^2

SMOG2 HLT2 line for K^0_S

Hlt2IFTFull_SMOG2KS2PiPiLL
prescale $= 0.02$
persistreco $=$ True
$\chi^2_{\text{DOF}}(\text{Track}) < 5$
$\chi^2_{\text{IP}}(\text{BPV}) > 25$
$m(\pi^+\pi^-) > (497.7 - 50)$ MeV/c^2
$m(\pi^+\pi^-) < (497.7 + 50)$ MeV/c^2
apt > 0 MeV/c
$\chi^2_{\text{DOF}}(v) < 25.0$
$\text{EV}_z < 2200$ mm
$\chi^2(\text{BPVVD}) > 0$
$t_{\text{life}}(\text{BPV}) > 0$ ns
$\chi^2_{\text{IP}}(\text{Parent}) < 75$
VetoWindow$(\Lambda^0) = 9$ MeV/c^2

SMOG2 sprucing line for Λ^0

smog2_L02ppi_ll_spruceline
prescale $= 1$
persistreco $=$ False
$p(\Lambda^0) > 2$ GeV/c
χ^2_{DOF}(Track) < 5
χ^2_{IP}(BPV) > 25
$m(p\pi) > (1115.683 - 25)$ MeV/c^2
$m(p\pi) < (1115.683 + 25)$ MeV/c^2
apt > 0 MeV/c
$\chi^2_{\text{DOF}}(v) < 25.0$
EV$_z < 2200$ mm
χ^2(BPVVD) > 0
t_{life}(BPV) > 0 ns
χ^2_{IP}(Parent) < 100
VetoWindow(K^0_S) $= 20$ MeV/c^2

SMOG2 sprucing line for K^0_S

smog2_ks2pipi_ll_spruceline
prescale $= 1$
persistreco $=$ False
$p(K^0_S) > 2$ GeV/c
$\chi^2_{\text{DOF}}(\text{Track}) < 5$
$\chi^2_{\text{IP}}(\text{BPV}) > 25$
$m(\pi^+\pi^-) > (497.7 - 50)$ MeV/c^2
$m(\pi^+\pi^-) < (497.7 + 50)$ MeV/c^2
apt > 0 MeV/c
$\chi^2_{\text{DOF}}(v) < 25.0$
$\text{EV}_z < 2200$ mm
$\chi^2(\text{BPVVD}) > 0$
$t_{\text{life}}(\text{BPV}) > 0$ ns
$\chi^2_{\text{IP}}(\text{Parent}) < 75$
VetoWindow$(\Lambda^0) = 9$ MeV/c^2

Leakage check

- Ensure data sample consists of candidates originating from pNe collisions
- Bunchcrossing type: Information whether bunches are empty or not during crossing
- Compared distributions of various variables with bunchcrossing type 1 and 3 in all bins of p_T and y^*
- Found no significant differences in the distributions in all bins
  →no visible leakage of Λ^0 or K_S^0 from pp

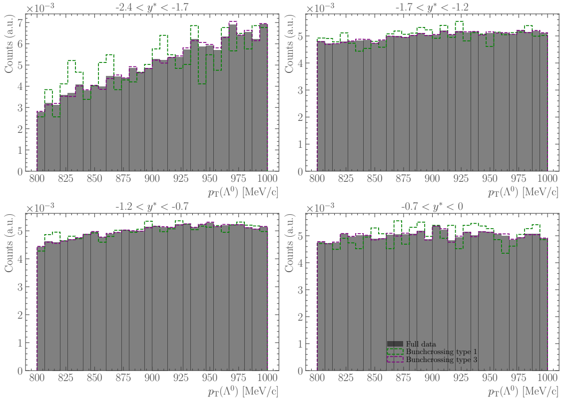

Multiplicity reweighting in ppNe simulation

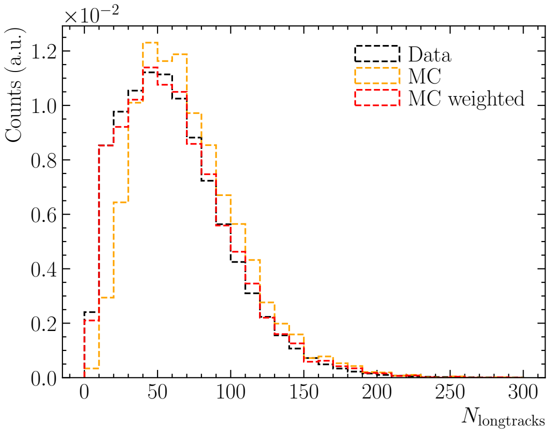

Tracking weights from pp calibration sample

- pp calibration sample with two muons in final state
- Tag-and-probe method
- Replace with SMOG2 specific tracking weights in future

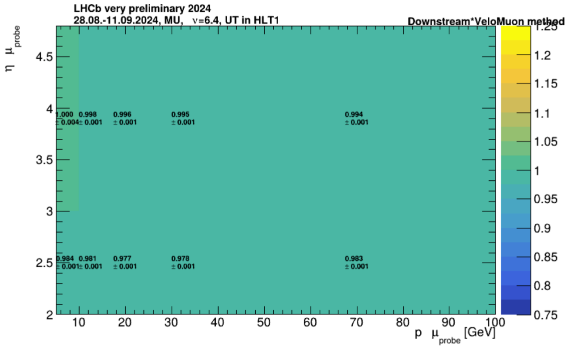

Trigger and reconstruction efficiencies

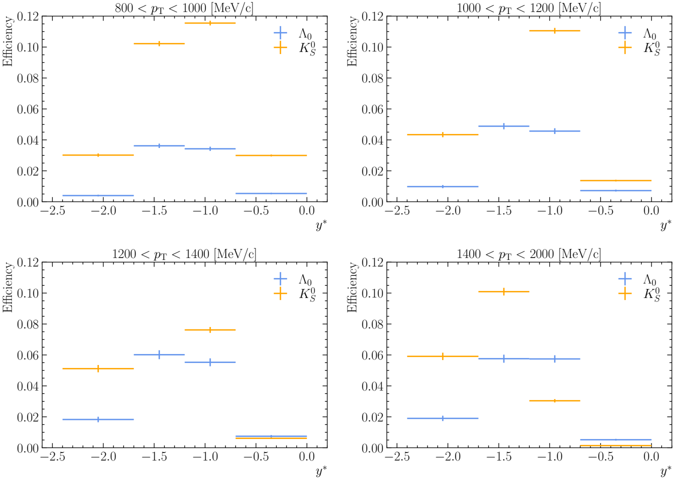

Selection efficiencies

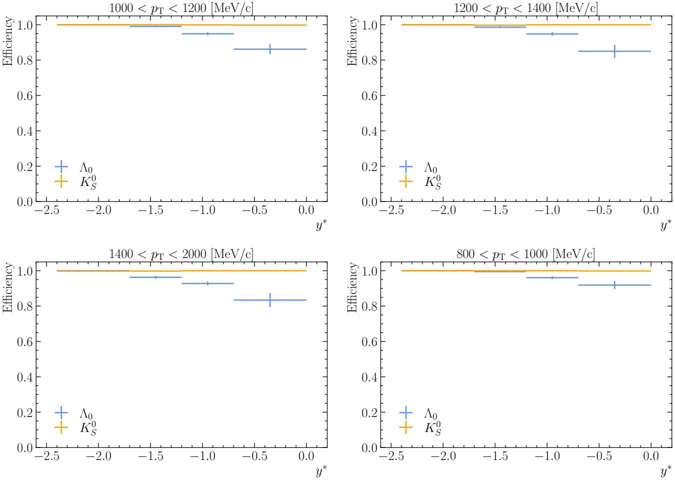

$\Lambda^0/\bar{\Lambda}^0$ ratio using ppNe simulation

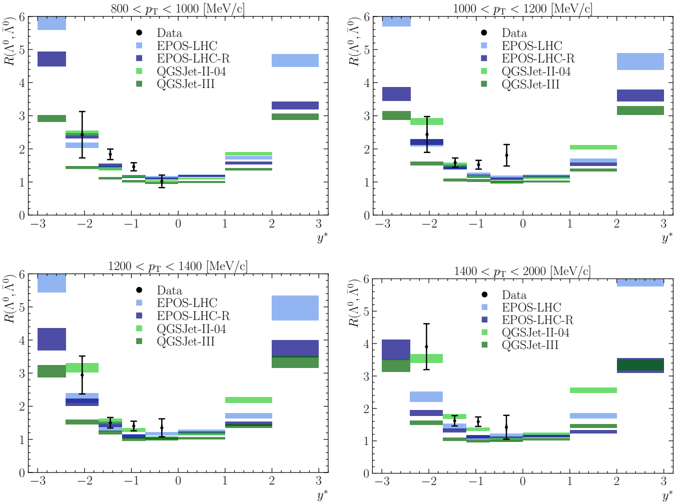

$\Lambda^0/\mathrm{K}^0_\mathrm{S}$ ratio in bins of p_T and ϕ

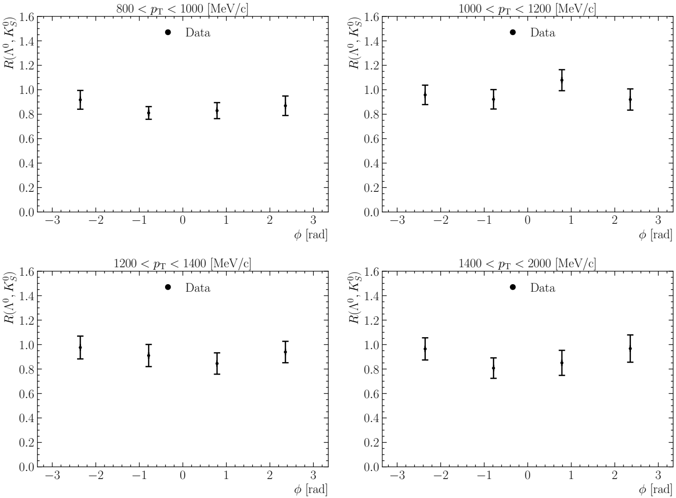

Stability check

- Perfrom analysis in bins of polar angle ϕ
- New 2D binning schemes: p_{T} and ϕ, y^* and ϕ
- Expect ratio to be independent of ϕ
- Results show no significant ϕ dependence

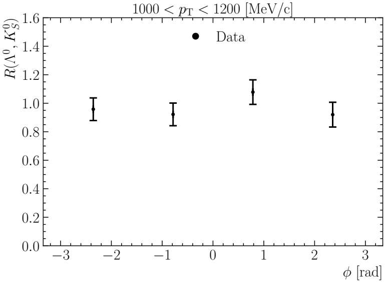

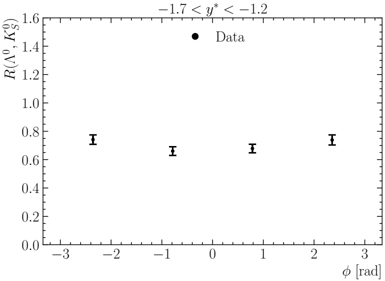

Stablility check: $\Lambda^0/\mathrm{K}^0_\mathrm{S}$ ratio in bins of y^* and ϕ